Optical properties of AIE organic chromophores embedded erbium-doped glass composites fabricated by spark plasma sintering

Mengmeng Meng, Panyi Wang, Yuchao Yuan, Muzhi Cai, Laurent Calvez, Jean Rocherullé, Hongli Ma, Junjie Zhang, Shiqing Xu, Xianghua Zhang

Optical properties of AIE organic chromophores embedded erbium-doped glass composites fabricated by spark plasma sintering

Mengmeng Meng[a], Panyi Wang[a], Yuchao Yuan[b], Muzhi Cai[a,*], Laurent Calvez[c], Jean Rocherulle[c], Hongli Ma[c], Junjie Zhang[a], Shiqing Xu[a], Xianghua Zhang[c]

[a] Key Laboratory of Rare Earth Optoelectronic Materials and Devices of Zhejiang Province, Institute of Optoelectronic Materials and Devices, China Jiliang University, Hangzhou 310018, China
[b] Jiangsu Key Laboratory of New Drug Research and Clinical Pharmacy, School of Pharmacy, Xuzhou Medical University, Xuzhou 221004, China
[c] ISCR (Institut des Sciences Chimiques de Rennes) UMR 6226, Univ Rennes, CNRS, F35000 Rennes, France
*Corresponding author: caimuzhi@cjlu.edu.cn

Keywords: SPS, AIE, Energy transfer, Rare earth ions

Encapsulation strategies can isolate the organic chromophores and prevent chemical or photochemical degradation. Inorganic transparent glass matrix has excellent utility as encapsulation matrices. Although the sol-gel method can make this encapsulation, the unclear sol-gel synthetic mechanism limits the synthesis of multi-component glass whose properties can be modified. A novel technique to encapsulate organic chromophores within multi-component glasses is required. In this letter, an organic chromophore was successfully encapsulated within a multi-component glass matrix by spark plasma sintering (SPS). The glass composite has great chemical and photochemical stability. Besides, a non-radiative energy transfer process between rare earth ions and organic chromophores was observed in the glass composites. These results indicate that the glass composite has great potential for optical application, and SPS can be a novel technique for encapsulating organic chromophores.

1. Introduction

Organic chromophores are widely used as active ingredients in semiconducting materials, solar energy cells, photonics, and various approaches to photodynamic therapy[1-3]. A potential drawback with conventional organic chromophores is their tendency to aggregate, which quenches the photoluminescence. Fortunately, research into organic emitters with aggregation-induced emission (AIE) properties has resolved this issue[4, 5]. Another common limitation of organic chromophores, especially those with long-wave-length absorption bands, is their susceptibility to chemical and photochemical degradation[6]. In principle, encapsulation strategies can attenuate this problem by isolating the organic molecules and preventing chemical or photochemical degradation[7].

Inorganic molecular sieves with three-dimensional lattices or networks have utility as porous encapsulation matrices[8]. They are compatible with various photochemical studies and have strong mechanical, chemical, and thermal stabilities. Many researchers have attempted to encapsulate organic chromophores within an inorganic medium to enhance their stability towards external stimuli. The organic chromophores composite inorganic glass has gotten a lot of interest because inorganic glass matrices offer strong mechanical, chemical, and thermal stabilities and high UV absorption, which can prevent photochemical destruction of the organic chromophores inside. However, achieving this kind of encapsulation is difficult because of the much higher synthesis temperature of an inorganic glass compared to that of organic chromophores. Although the sol-gel method can make this encapsulation, the unclear sol-gel synthetic mechanism of multi-component glasses limits its further application. As a result, a novel approach for encapsulating the organic emitter within the multi-component glass matrix is necessary.

Recently, we discovered that it is possible to incorporate an organic chromophore within an inorganic oxide glass matrix through spark plasma sintering technology (SPS)[9]. However, the universality of the encapsulation process and the optical properties of the glass composites were not investigated further in that study. In this work,

another organic chromophore with AIE property (denoted as DBP-BTO) was encapsulated inside an inorganic non-oxide glass matrix (ZrF_4-BaF_2-LaF_3-AlF_3-NaF, ZBLAN) by SPS. The optical properties and UV resistance of the DBP-BTO composite ZBLAN glass were analyzed. Besides, the energy transfer process between DBP-BTO and rare earth ions was also investigated based on the photoluminescence spectra (PL) and the PL decay curves.

2. Experimental section

2.1 Synthesis step

Firstly, DBP-BTO molecules were dissolved in separate solutions of Tetrahydrofuran (THF) at 1 mg ml^{-1}. Then, the solution was diluted in a beaker, and 1.5 g of ZBLAN glass powder was weighed into the diluted solution. Afterward, the beaker was put in a drying oven at around 70 °C to dry for 2 h. After drying, the mixed powder was placed in the agate mortar to grind for better sample homogeneity. Finally, the samples were prepared by introducing glass powder into a carbon die with an aluminum foil in the inner part of the die as a carbon diffusion barrier. The glass powder was sintered under vacuum by Spark Plasma Sintering. Maximum pressure of 0.5 t was applied. A temperature of 253 °C was obtained for about 6 min, and the temperature was kept for 5 min. After polishing, the corresponding various performance tests were carried out.

2.2 Characterization

The photoluminescence (PL) spectra of samples were obtained on an FL3-211 type spectrometer (JOBIN YVON, France). The absorption spectrum of ZBLAN-Er and DBP-ZBLAN-Er were tested by a UV-Vis spectrophotometer (PE lambda 950). Time-resolved PL spectra were obtained by the time-correlated single-photon counting method using the FLS1000 equipped with a 375 nm pulsed laser. The temperature-dependent emission spectra were measured by EX-100 equipped with 150 W pulsed xenon lamps as an excitation source. The DSC scans (NETZSCH DSC 3500) were carried out on samples of 10.2 mg in an Al pan. The glass transition temperature was determined at a heating rate of 10 K/min.

3. Results and discussion

Firstly, to optimize the sintering process, the thermal characteristics of the ZBLAN glass host and DBP-BTO chromophore were studied. The structure of DBP-BTO is shown in Fig. 1(a)[10]. The DSC curve reveals the T_g (262 ℃) of the ZBLAN glass matrix, as shown in Fig. 1(b). The thermogravimetric (TG) curve demonstrates that when heated to 380 °C, DBP-BTO begins to decompose, and when heated further to 449 °C, DBP-BTO loses 26.8% of its weight. Because of the high degradation temperature of DBP-BTO, it can be incorporated into a wider range of glass matrices. Based on the optimal sintering parameters, four DBP-BTO composited ZBLAN glasses with different DBP-BTO concentrations were synthesized, denoted as DBP-ZBLAN-X (X=1, 2, 3, 4).

The prepared DBP-ZBLAN-X series glasses show strong PL under UV excitation, as shown in the inset of Fig. 1(a), which suggests the structure of the organic chromophore was not destroyed during the SPS process. Fig. 1(c) shows the PL spectra of DBP-ZBLAN-X series glass composites at an excitation wavelength of 365 nm. It is evident that with an increase in the content of the DBP-BTO, the PL intensity of glass composites gradually increases, demonstrating the AIE nature of DBP-BTO. As aggregates form, the intramolecular rotations are restricted by spatial constraints from neighboring molecules. Therefore, the nonradiative decay is blocked, and the PL intensity is enhanced. However, with the increase in concentration, the glass composite shows red-shifted PL peaks. This phenomenon may result from varied molecular alignments and intermolecular interactions. Fig. 1(d) shows the normalized PL spectrum of DBP-ZBLAN-3, and the corresponding inset gives the PL intensity with excitation wavelength correlation, respectively. It is also discovered that for all DBP-ZBLAN-X series glasses, the normalized PL spectra show the same shape when the excitation wavelength is changed from 365 nm to 405 nm. Such similar features of PL spectra at different excitation wavelengths indicate that the cyan emission originates from recombining the same excited state[11-13]. The inset suggests that the glass composites exhibit emission dependence on

the excitation wavelengths. We speculate that this phenomenon may be due to the scattering effect caused by the aggregation of DBP-BTO chromophores[14].

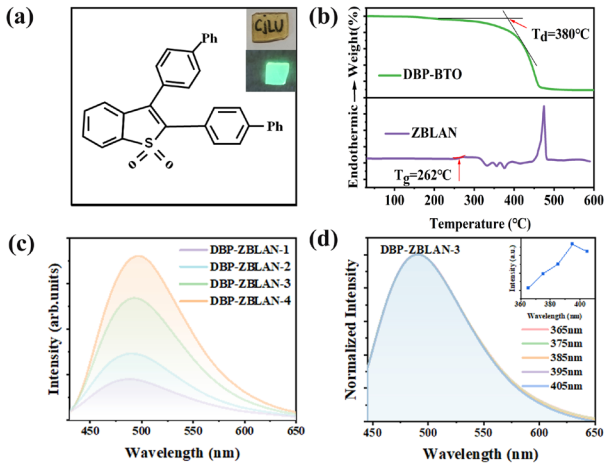

Fig. 1. (a) The structure of DBP-BTO (the insets show the pictures of DBP-ZBLAN-3). (b) TG and DSC curves of DBP-BTO and ZBLAN glass. (c) The PL spectra of glass samples with different DBP-BTO doping concentrations. (d) The normalized PL spectra of DBP-ZBLAN-3 excited by different wavelengths of light (the inset shows the corresponding PL intensities).

Fluorescence thermal quenching performance tests on DBP-ZBLAN-X series glass composites were undertaken because thermal stability is an essential criterion for luminescent materials. Fig. 2(a) depicts the temperature-dependent PL spectra of DBP-ZBLAN-3 under 365 nm excitation in the temperature range of 304 K to 424 K. During the heating process, the PL intensity of DBP-ZBLAN-3 drops as the temperature rises, which is caused by the thermal quenching process as the energy of the excited state is converted back to the ground state through non-radiative conversion[15-18]. Simultaneously, the PL peak shows a slightly blue shift as the temperature increasing, which is probably attributed to thermally activated phonon-assisted tunneling[19]. Fig. 2(b) displays the PL intensity of the DBP-ZBLAN-3 sample with heating temperature correlation. It is clear that the sample can still maintain more than half of the initial PL intensity when heated to 425 K.

The UV resistance of both DBP-BTO powders and glass composite was also performed. The DBP-BTO solid powders were isostatically pressed into wafers of the same thickness as the DBP-ZBLAN-3 sample. Then both samples were placed under a 365 nm UV lamp to observe the photochemical degradation of each, and the corresponding PL spectra were measured every 30 h, and the results are shown in Fig. 2(c-d). The PL intensity of both the DBP-BTO wafer and DBP-ZBLAN-3 sample decreased with increasing irradiation time. The DBP-BTO wafer hardly showed luminescence after 30 h, while the PL intensity of the DBP-ZBLAN-3 sample dropped to 33.3% of the initial value after 60 h. The result demonstrates that the ZBLAN glass matrix can protect the DBP-BTO from UV radiation.

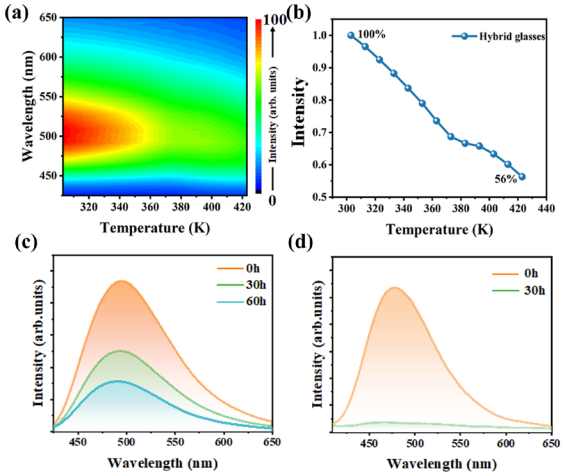

Fig. 2. (a) The temperature-dependent PL spectra of DBP-ZBLAN-3. (b) Correlation between PL intensity and heating temperature of DBP-ZBLAN-3. The PL spectra of (c) DBP-ZBLAN-3 and (d) DBP-BTO wafer after irradiation under UV lamp.

Plus, it would be interesting to explore the luminescence properties of DBP-BTO composited trivalent lanthanide ions doped glass matrix because organic-inorganic hybrids incarcerating trivalent lanthanide ions are a very promising class of materials[20]. Thus, the DBP-BTO composite Er^{3+} doped ZBLAN glass (denoted as DBP-ZBLAN-Er) was synthesized. Fig. 3(a) depicts the absorption spectra of DBP-ZBLAN-Er and Er^{3+} doped ZBLAN glass (denoted as ZBLAN-Er) in the 400-1100 nm range. Absorption bands in this figure are labeled, corresponding to the transitions starting from the Er^{3+}: $^4I_{15/2}$ ground state to higher $^4I_{12/2}$, $^4I_{9/2}$, $^4F_{9/2}$, $^4S_{3/2}$, $^2H_{11/2}$, $^4F_{7/2}$, levels. Although the shape

of the absorption peaks of Er^{3+} ions seems to be changed because of the effect of DBP-BTO, the position of the absorption peak hardly changes in both samples. It is also noted that the absorption peak intensity of Er^{3+} ions of the DBP-ZBLAN-Er sample is weaker than that of the ZBLAN-Er sample, which is probably caused by the scattering introduced by DBP-BTO chromophores. Fig. 3(b) shows the upconversion luminescence spectra of the ZBLAN-Er and the DBP-ZBLAN-Er samples excited by 980 nm LD. It is shown that the PL intensity of ZBLAN-Er is stronger than that of DBP-ZBLAN-Er since ZBLAN-Er has a more efficient absorption process, as discussed above. However, the possible energy transfer process between Er^{3+} ions to DBP-BTO chromophores may also quench the PL of Er^{3+} as well.

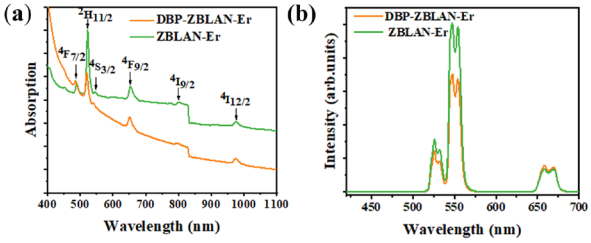

Fig. 3. (a) The absorption spectra of ZBLAN-Er and DBP-ZBLAN-Er. (b) the upconversion PL spectra of ZBLAN-Er and DBP-ZBLAN-Er excited by 980 nm LD.

Thus, to confirm the existence of the energy process between Er^{3+} ions and DBP-BTO chromophores, the down-shifting PL spectra of the ZBLAN-Er and the DBP-ZBLAN-Er samples were performed. Fig. 4(a) and 4(b) show the PL spectrum of the ZBLAN-Er and DBP-ZBLAN-Er samples excited by 280 and 375 nm light, respectively. It suggests that the ZBLAN-Er sample can not be efficiently excited by 280 nm light, while the DBP-ZBLAN-Er sample can be efficiently excited by both 280 nm and 375 nm light. Since both DBP-BTO and Er^{3+} can be excited by 375 nm light, the PL spectrum of DBP-ZBLAN-Er shows the combined shape of the spectrum of Er^{3+} ions and DBP-BTO chromophores. Interestingly, two negative peaks were observed around 475 nm and 525 nm, associated with Er^{3+}: $^4I_{15/2} \rightarrow {}^4F_{7/2}$ and $^4I_{15/2} \rightarrow {}^2H_{11/2}$ transition, respectively, as shown in Fig. 4(c). This confirms an energy transfer process between DBP-BTO and Er^{3+} ions. Fig. 4(d) contrasts the normalized PL spectrum of DBP-ZBLAN-3 and DBP-ZBLAN-Er under 280 nm excitation. The typical green light from Er^{3+} ions was observed, as marked in Fig. 4(d), which suggests that DBP-BTO can sensitize Er^{3+}.

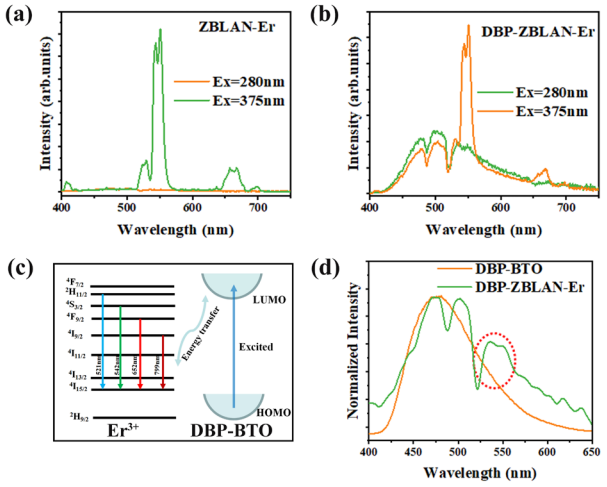

Fig. 4 The PL spectra of ZBLAN-Zr (a) and DBP-ZBLAN-Er (b) sample excited by 280 and 375 nm light. (c) the possible energy transfer sketch of Er^{3+} and DBP-BTO. (d) The normalized PL spectra of DBP-BTO and DBP-ZBLAN-Er excited by 280 nm light.

Fig. 5(a) displays that the luminescence lifetime of the DBP-BTO chromophore at 495 nm is around 2.3 ns, which is close to the value in reference[10]. In order to distinguish whether the energy transfer process is radiative or non-radiative, the PL decay curves of ZBLAN-Zr and DBP-ZBLAN-Er samples at different wavelengths were investigated, as shown in Fig. 5(b-c). Fig. 5(b) demonstrates that the luminescence lifetime of all the visible wavelengths of Er^{3+} ions in the ZBLAN-Er sample is around 10^{-1} ms. Meanwhile, the luminescence lifetime of all the visible wavelengths of Er^{3+} ions in DBP-ZBLAN-Er is dropped by five orders of magnitude to the ns level. Although the detailed energy transfer process in the DBP-ZBLAN-Er sample is unclear, the results confirm that the energy process between DBP-BTO chromophores and Er^{3+} ions is a non-radiative process. There are two mechanisms of a non-radiative process, Förster resonance energy transfer (FRET) and direct

electron exchange transfer (DET), as shown in Fig. 5(d). However, it is difficult to distinguish the mechanism for the energy transfer process in DBP-ZBLAN-Er glass. Considering the distribution of the organic chromophores in the glass matrix, usually the cluster[9], with sizes from 10 to 100 nm, the DET is more likely to happen. More work needs to be done to address this issue.

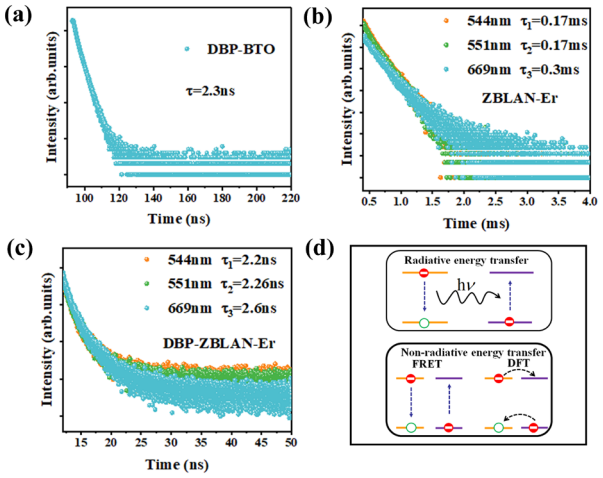

Fig. 5 The decay PL curves at different wavelengths of DBP-BTO (a), ZBNLAN-Er (b), and DBP-ZBLAN-Er (c) under 375 nm excitation. (d) Schematic presentations of radiative and non-radiative (FRET and DET mechanisms) energy transfer.

4. Conclusion

In conclusion, the organic chromophore DBP-BTO has been successfully encapsulated within the ZBLAN glass matrix through SPS technology. The PL intensity of the DBP-BTO composite glass keeps improving with the increase of DBP-BTO (37-667 ppm). Besides, the temperature-dependent PL and UV resistance test suggest that the DBP-BTO composite glass has great luminescence thermal stability and UV resistance. Moreover, the PL spectra and luminescence lifetime of the DBP-ZBLAN-Er sample confirm the existence of the energy transfer process between Er^{3+} ions and DBP-BTO, and this energy transfer process is a non-radiative energy transfer process. These experimental results indicate that SPS technology may become an emerging technology for synthesizing organic-inorganic glass composites. This kind of glass composites may have many potential applications in optics.

Acknowledge.

This work was supported by Natural Science Foundation of Zhejiang Province (Q21F050026); The Fundamental Research Funds for the Provincial Universities of Zhejiang (2022YW32); National Key Research and Development Project of China (2018YFE0207700); National Natural Science Foundation of China Joint Fund Project (U1909211).
Mengmeng Meng and Panyi Wang contribute equally.

References

[1] S.F.H. Correia, V. de Zea Bermudez, S.J.L. Ribeiro, P.S. André, R.A.S. Ferreira, L.D. Carlos, Luminescent solar concentrators: challenges for lanthanide-based organic–inorganic hybrid materials, J. Mater. Chem. A, 2 (2014) 5580-5596.
[2] S.H. Mir, L.A. Nagahara, T. Thundat, P. Mokarian-Tabari, H. Furukawa, A. Khosla, Review—Organic-Inorganic Hybrid Functional Materials: An Integrated Platform for Applied Technologies, J Electrochem Soc, 165 (2018) B3137-B3156.
[3] H. Mustroph, M. Stollenwerk, V. Bressau, Current developments in optical data storage with organic dyes, Angew Chem Int Ed Engl, 45 (2006) 2016-2035.
[4] Y. Chen, J.W.Y. Lam, R.T.K. Kwok, B. Liu, B.Z. Tang, Aggregation-induced emission: fundamental understanding and future developments, Mater Horizons, 6 (2019) 428-433.
[5] Y. Hong, J.W.Y. Lam, B.Z. Tang, Aggregation-induced emission, Chem Soc Rev, 40 (2011).
[6] A.P. Demchenko, Photobleaching of organic fluorophores: quantitative characterization, mechanisms, protection, Methods Appl Fluoresc, 8 (2020) 022001.
[7] B.K. Shaw, A.R. Hughes, M. Ducamp, S. Moss, A. Debnath, A.F. Sapnik, M.F. Thorne, L.N. McHugh, A. Pugliese, D.S. Keeble, P. Chater, J.M. Bermudez-Garcia, X. Moya, S.K. Saha, D.A. Keen, F.X. Coudert, F. Blanc, T.D. Bennett, Melting of

hybrid organic-inorganic perovskites, Nat Chem, 13 (2021) 778-785.
[8] J. Maillard, K. Klehs, C. Rumble, E. Vauthey, M. Heilemann, A. Furstenberg, Universal quenching of common fluorescent probes by water and alcohols, Chem Sci, 12 (2020) 1352-1362.
[9] M. Cai, L. Calvez, J. Rocherulle, P.-a. Bouit, M. Hissler, H. Ma, C. Roiland, V. Dorcet, J. Zhang, S. Xu, X. Zhang, Aggregation-induced emission fluorophore doped phosphate glass: Toward light-emitting electrochemical cells, J. Alloys Compd, 897 (2022).
[10] J. Guo, S. Hu, W. Luo, R. Hu, A. Qin, Z. Zhao, B.Z. Tang, A novel aggregation-induced emission platform from 2,3-diphenylbenzo[b]thiophene S,S-dioxide, Chem Commun (Camb), 53 (2017) 1463-1466.
[11] J.J. Luo, X.M. Wang, S.R. Li, J. Liu, Y.M. Guo, G.D. Niu, L. Yao, Y.H. Fu, L. Gao, Q.S. Dong, C.Y. Zhao, M.Y. Leng, F.S. Ma, W.X. Liang, L.D. Wang, S.Y. Jin, J.B. Han, L.J. Zhang, J. Etheridge, J.B. Wang, Y.F. Yan, E.H. Sargent, J. Tang, Efficient and stable emission of warm-white light from lead-free halide double perovskites, Nature, 563 (2018) 541-545.
[12] Z.F. Tan, J.H. Li, C. Zhang, Z. Li, Q.S. Hu, Z.W. Xiao, T. Kamiya, H. Hosono, G.D. Niu, E. Lifshitz, Y.B. Cheng, J. Tang, Highly Efficient Blue-Emitting Bi-Doped Cs_2SnCl_6 Perovskite Variant: Photoluminescence Induced by Impurity Doping, Adv. Funct. Mater., 28 (2018) 10.
[13] L. Zhou, J.F. Liao, Z.G. Huang, J.H. Wei, X.D. Wang, H.Y. Chen, D.B. Kuang, Intrinsic Self-Trapped Emission in 0D Lead-Free $(C_4H_{14}N_2)(2)In_2Br_{10}$ Single Crystal, Angew. Chem.-Int. Edit., 58 (2019) 15435-15440.
[14] L. Zou, X. Qin, H. Sun, S. Wang, W. Ding, Y. Liu, C. Wei, B. Jiang, Y. Gong, Room-temperature phosphorescent polymers with excitation-wavelength and delay-time emission dependencies, RSC Advances, 9 (2019) 36287-36292.
[15] C. Yang, X. Liang, X. Di, P. Li, G. Hu, R. Cao, W. Xiang, Facile fabrication and luminescence characteristics of Ce:YAG phosphor glass thick films coated on a glass substrate for white LEDs, Ceram Int, 42 (2016) 14526-14532.
[16] Y. Zhang, Z. Zhang, X. Liu, G. Shao, L. Shen, J. Liu, W. Xiang, X. Liang, A high quantum efficiency $CaAlSiN_3:Eu^{2+}$ phosphor-in-glass with excellent optical performance for white light-emitting diodes and blue laser diodes, Chem Eng J, 401 (2020).
[17] Q.-Q. Zhu, X. Xu, L. Wang, Z.-F. Tian, Y.-Z. Xu, N. Hirosaki, R.-J. Xie, A robust red-emitting phosphor-in-glass (PiG) for use in white lighting sources pumped by blue laser diodes, J. Alloys Compd, 702 (2017) 193-198.
[18] J. Huang, X. Hu, J. Shen, D. Wu, C. Yin, R. Xiang, C. Yang, X. Liang, W. Xiang, Facile synthesis of a thermally stable $Ce^{3+}:Y_3Al_5O_{12}$ phosphor-in-glass for white LEDs, CrystEngComm, 17 (2015) 7079-7085.
[19] M. Que, Z. Ci, Y. Wang, G. Zhu, S. Xin, Y. Shi, Q. Wang, Crystal structure and luminescence properties of a cyan emitting $Ca_{10}(SiO_4)_3(SO_4)_3F_2:Eu^{2+}$ phosphor, CrystEngComm, 15 (2013).
[20] J. Wang, R. Deng, Energy Transfer in Dye-Coupled Lanthanide-Doped Nanoparticles: From Design to Application, Chem Asian J, 13 (2018) 614-625.